Energy Technology: Generation, Coversion, Storage, Distribution, Volume 6, Issue 9, pp.1777-1787
DOI: 10.1002/ente.201700894

Compatibility of NiO/CuO in Ca-Cu Chemical Looping for High-Purity H_2 Production with CO_2 Capture

Lili Tan [a], Changlei Qin [a,] Zhonghui Zhang [a], Jingyu Ran [a], and Vasilije Manovic [b]*

[a] Key Laboratory of Low-grade Energy Utilization Technologies and Systems of Ministry of Education, College of Power Engineering, Chongqing University, Chongqing 400044, China

[b] Combustion and CCS Centre, Cranfield University, Cranfield, Bedfordshire MK43 0AL, United Kingdom

[*] Corresponding author:

Tel.: +86-23-65103101. Email: c.qin@cqu.edu.cn.

ABSTRACT

Ca-Cu chemical looping is a novel and promising approach in converting methane into pure H_2 following the principle of sorption-enhanced reforming. Its operational efficiency is largely determined by an appropriate coexistence of Cu-based oxygen carriers and Ni-based catalysts. In this work, bifunctional NiO/CuO composites were synthesized and their catalytic activity for H_2 production was measured using a fixed-bed reactor system equipped with an online gas analyzer. It is reported for the first time that the presence of CuO, even in a small amount (1 wt.%), could seriously hinder the activity of Ni-based catalysts in H_2 production, and experimental results show that the negative effect of doping CuO is strengthened with increasing CuO content and calcination temperature during sample preparation. With the help of a series of specific test and characterization techniques (SEM-EDS, BET, XRD, TPR and XPS), interaction rules between NiO and CuO was further investigated and understood, and based on that an action mechanism model was proposed. Furthermore, an arrangement of mixed particles that avoiding the intimate contact of CuO/NiO was suggested and tested, and a superior performance was demonstrated while observing no restrictions of CuO on Ni-based catalysts in sorption-enhanced steam-methane reforming under the conditions of Ca-Cu chemical looping.

Keywords: Ca-Cu chemical looping, hydrogen production, Ni/Cu interaction, CO_2 capture

1. Introduction

Hydrogen plays an important role in modern industry. It is an important chemical raw material in synthesizing ammonia and methanol, and for hydrogenation. Also it is seen as a fuel of the future with the advantages of high calorific value and nonpolluting. Currently, hydrogen is mainly produced from methane by the methods of steam reforming, auto-thermal reforming, partial oxidation, CO_2 reforming and catalytic decomposition. Of these, steam methane reforming (SMR) is the most widely adopted industrial process owing to its high economic efficiency.[1] SMR consists of two major steps: the catalytic steam reforming of CH_4 (Eq. 1) with the production of CO and H_2 at high temperature (800-900°C); and the water gas shift reaction (Eq. 2) at low temperature (180-350°C). However, the application of SMR is largely limited by reaction equilibrium, and rigorous reaction conditions and costly equipment are inevitable in industry.[2] In contrast, sorption-enhanced steam methane reforming (SE-SMR) could overcome the aforementioned limitations with the addition of the carbonation reaction of Eq. 3. As a result, the hydrogen production process is achieved in one comprehensive step as seen of Eq. 4. In this case, not only are the chemical equilibria of Eqs. 1-2 broken and reactions are promoted to move in the forward direction according to Le Chatelier's principle, but the heat required in SMR is partially met by Eq. 3, which is a highly exothermic reaction.

$$CH_4 + H_2O \leftrightarrow CO + 3H_2 \qquad \Delta H^0_{298K} = 206\,kJ/mol \qquad (1)$$

$$CO + H_2O \leftrightarrow CO_2 + H_2 \qquad \Delta H^0_{298K} = -41\,kJ/mol \qquad (2)$$

$$CO_2 + CaO \leftrightarrow CaCO_3 \qquad \Delta H^0_{298K} = -178\,kJ/mol \qquad (3)$$

$$CH_4 + 2H_2O + CaO \leftrightarrow CaCO_3 + 4H_2 \qquad \Delta H^0_{298K} = -13\,kJ/mol \qquad (4)$$

To realize the multicycle operation required of SE-SMR for H_2 production, it is necessary to regenerate CO_2 sorbent by calcining the $CaCO_3$ formed.[3] Lyon et al. were the first proposing a second chemical loop in calcium looping, and using the exothermic oxidation of Fe to FeO to support the calcination step. However, the reduction of FeO back to Fe is endothermic and Fe/FeO chemical

loop could cause N_2 to be mixed in the flue gas, leading to difficulty in carbon capturing.[4] To solve these problems, Abanades et al. proposed a more effective process that utilizes the chemical looping of CuO/Cu (Eqs. 5-6) to supply energy for calcining $CaCO_3$, termed Ca-Cu chemical looping. As shown in Figure 1.[5] The system contains 3 steps: (1) hydrogen production by SE-SMR, (2) spontaneous exothermic Cu oxidation with air, and (3) simultaneous $CaCO_3$ calcination and CuO reduction with a fuel gas.

$$CH_4 + 4CuO \leftrightarrow 4Cu + CO_2 + 2H_2O \qquad \Delta H^0_{298K} = -179.4 kJ/mol \qquad (5)$$

$$2Cu + O_2 \leftrightarrow 2CuO \qquad \Delta H^0_{298K} = -156 kJ/mol \qquad (6)$$

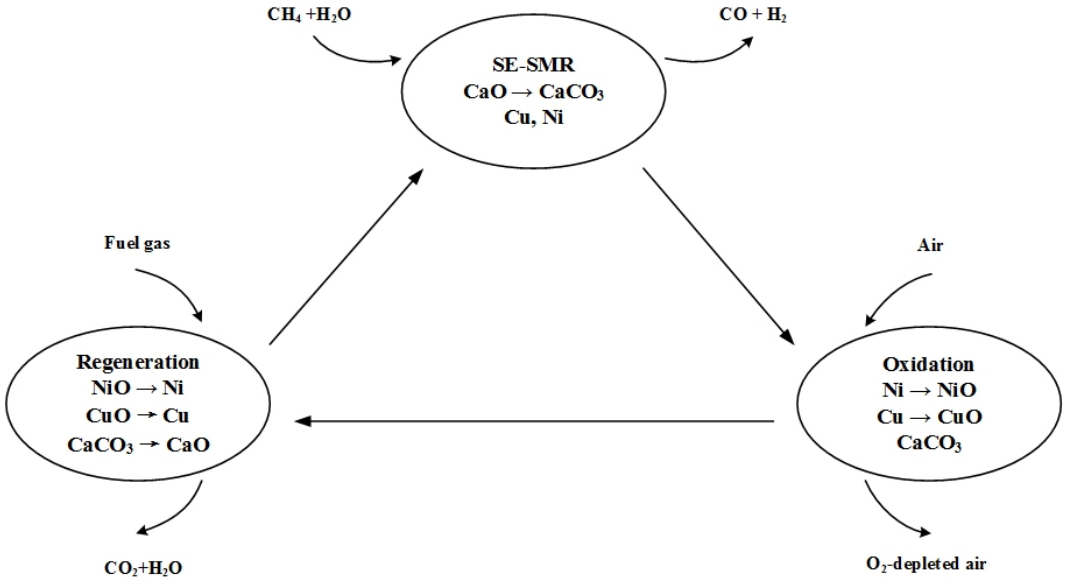

Figure 1. Schematic of Ca-Cu chemical looping for hydrogen production.[5]

Initial research on Ca-Cu chemical looing was carried out through simulation. Fernández presented simulation work on the reforming reaction and Cu oxidation within the boundary conditions of the Ca-Cu looping process and studied impacts of temperature, pressure, O_2 content and copper substrate reactivity, proving the feasibility of the concept.[6] García-Lario et al. investigated the reduction kinetics of a high-CuO-loaded pellet suitable for Ca-Cu chemical looping and pointed out that both H_2 and CO had additive effects on the reaction rate.[7] Qin et al. studied the simultaneous reduction of CuO and decomposition of $CaCO_3$ in an adiabatic fixed-bed reactor operating at 1 atm by

developing a dynamic model and, then in further studies, a mathematical model was developed considering reactions, and mass and heat transfer inside a spherical particle composed of uniformly-distributed CuO and $CaCO_3$ grains, or a core-in-shell form with CuO as core and $CaCO_3$ as shell. It was suggested that the addition of steam and adopting a small $CaCO_3$ grain size could effectively avoid local overheating of the particles.[8, 9]

The pellets used in the Ca-Cu chemical looping hydrogen production process contain Ni-based catalysts, Cu-based oxygen carriers and Ca-based sorbents; thus it is a key point to fabricate, test, and obtain materials with good efficiency and stability that are suitable for the process. The individual Ni-based catalysts, Cu-based oxygen carriers or Ca-based sorbents have been widely studied.[10] The major challenge of Ni-based catalysts is fouling by coke deposition in the reforming reaction, and the combination of Ni with specific metal oxides can weaken this side effect.[11] CaO-based sorbents sinter easily in carbonation/calcination cycles,[12, 13] and the addition of inerts during the formation of the supporting framework could improve the cyclic stability.[14-17] CuO-based oxygen carriers also need a support for stable and effective operation, and the most promising performance has been demonstrated using alumina.[18, 19]

In contrast, research is presently insufficient on multi-functional materials including two or more of Ni-based catalysts, Cu-based oxygen carriers or Ca-based sorbents. Ni/Ca bifunctional catalyst/sorbent synthesized by impregnation methods was found to be less active in hydrogen generation than Ni/Al_2O_3.[20] Broda et al. synthesized a Ca−Ni bifunctional material derived from a hydrotalcite structure via a co-precipitation technique, and better H_2 production performance was observed than with limestone mixed with $Ni-SiO_2$ or a Ca-free, nickel hydrotalcite-derived catalyst.[21] $Ni/CaO-Ca_5Al_6O_{14}$ prepared by a sol-gel method also showed good activity and stability over 10 SE-SMR cycles.[22] These results indicate that Ni-based catalysts and Ca-based sorbents could exhibit good compatibility in bifunctional composites. Some research was also conducted on

the Ca-Cu bifunctional material. Manovic et al. synthesized a new class of material with a CaO/CuO core-in-shell structure with calcium aluminate cement as a support. It was confirmed that the composite material is suitable for the proposed cycles.[23] Qin et al. synthesized CaO/CuO sorbents supported with various selected precursors and evaluated the effect of thermal pre-treatment of copper precursor and steam addition on the cyclic reactivity of composite sorbents.[24, 25] The results show that all the composites have stable redox properties; however, CaO's loss-in-capacity problem was still observed, which is even more pronounced in the presence of CuO.

By reviewing the literature, it is clear that mutual effects between Ca-based sorbents and Ni-based catalysts or Cu-based oxygen carriers have been studied and understood. In fact, the compatibility between Ni-based catalysts and Cu-based oxygen carriers is probably more important. However, to the best of our knowledge, no such work has been reported. In this work, we first investigated the impact of Cu component on Ni-based catalysts and reported an interesting rapid loss of the catalytic activity for H_2 production. Then, a series of testing and characterization work was carried out to understand the interactive process and a mechanism was proposed. Finally, a co-existence form of Ni-based catalysts and Cu-based oxygen carriers was proposed and verified for practical application in the Ca-Cu chemical looping for hydrogen production process.

2. Experimental Section

2.1. Preparation of Cu/Ni Composite Material

Composite material with 50 wt.% CuO, 12 wt.% NiO and 38 wt.% Al_2O_3 was synthesized initially using a sol-gel method according to the following procedure: appropriate amounts of $Ni(NO_3)_2 \cdot 6H_2O$, $Cu(NO_3)_2 \cdot 3H_2O$, $Al(NO_3)_3 \cdot 9H_2O$ and distilled water were mixed. Then, the mixed nitrates were gradually added in a molar ratio of 1:2 to citric acid, with stirring at 100°C continued for 6 h. After hydrolysis, the obtained gel was dried at 110°C for 12 h and calcined at 650°C for 5 h. Interestingly,

almost no catalytic activity of Ni for the SMR process was observed in our initial tests for composites with high Cu content. Therefore, further work was conducted only on composites with a low Cu content in order to explore the potential interaction between NiO and CuO, and to arrange their co-existing structure such that it could be suitable for the Ca-Cu chemical looping process. Composites with low CuO content were prepared by the impregnation method. First, appropriate amounts of $Ni(NO_3)_2 \cdot 6H_2O$ and $Cu(NO_3)_2 \cdot 3H_2O$ were dissolved in 30 mL distilled water. Then, 4.7 mL mixed nitrate solution was added to 5 g nano γ-Al_2O_3 support, followed by ultrasonic vibration for 30 min, drying overnight at 110°C and calcination for 5 h in air. The prepared composites were abbreviated as CuxNi12, where x and 12 represent the mass fraction of CuO (0, 1, 3, 5 and 50 wt.%) and NiO, respectively. In the work, calcination temperature was fixed at 650°C during material preparation, except when its effect was specifically being studied.

2.2. Catalytic Test

SMR experiments were conducted in a fixed-bed reaction system as shown in Figure 2. The system consists of liquid and gas feeding sections, a fixed-bed reactor with a heated section and a gas product analysis section. The gas was fed from the bottom of the reactor and steam was generated by feeding liquid water via a syringe pump into a preheating furnace at 400°C. Flow rates of N_2, CH_4 and H_2 were controlled using mass flow controllers (MFC). The reactor, with an inner diameter of 22.4 mm, is constructed of quartz and contains a fritted quartz disc to support the catalyst. It was placed in a tubular furnace and the temperature of the bed was controlled by an N-type thermocouple. Gas product from the reactor was water-cooled and dried, and analyzed continuously using an online Nova syngas analyzer equipped with infrared detectors for CO, CO_2 and CH_4, and a thermal conductivity H_2 detector. In a typical experiment, 1 g catalyst (250−420 μm) was loaded in the reactor. Subsequently, the catalyst was reduced in a flow of 100 mL/min H_2 and 100 mL/min N_2 at 650°C for 1 h. After that, the SMR reaction was performed at 650°C using a flow of 40 mL/min CH_4 and 635.5 mL/min N_2. The steam-

to-methane molar ratio was kept at 4, and the reaction was held for 1 h in the work.

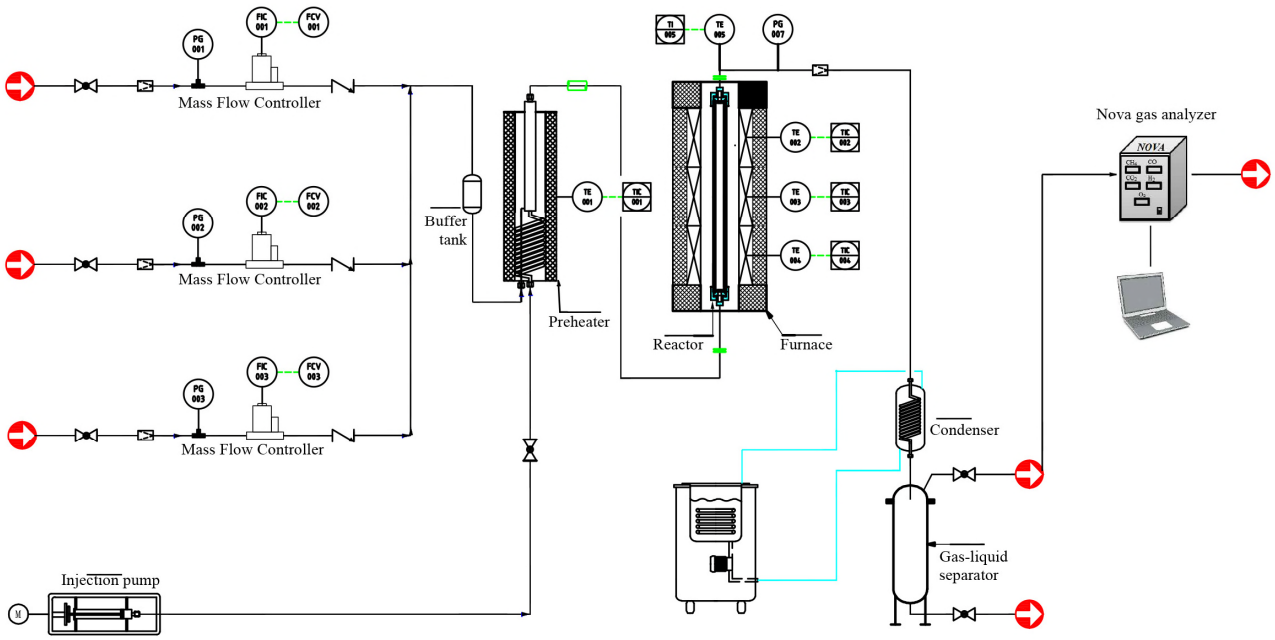

Figure 2. Schematic diagram of the fixed-bed reactor system for catalyst activity testing.

Methane conversion and gas selectivity were used to evaluate the activity of catalysts for H_2 production. Their values were calculated using the following equations:

$$\text{Methane conversion} = \frac{[CO]+[CO_2]}{[CH_4]+[CO]+[CO_2]} \cdot 100\% \quad (7)$$

$$\text{CO selectivity} = \frac{[CO]}{[H_2]+[CO_2]+[CO]} \cdot 100\% \quad (8)$$

$$CO_2 \text{ selectivity} = \frac{[CO_2]}{[H_2]+[CO_2]+[CO]} \cdot 100\% \quad (9)$$

$$H_2 \text{ selectivity} = \frac{[H_2]}{[H_2]+[CO_2]+[CO]} \cdot 100\% \quad (10)$$

where [CO], [CO_2], [CH_4], and [H_2] are the real-time values of their concentrations.

2.3. Material Characterization

Surface morphology of the materials was investigated using a TESCN VEGA 3 SBH scanning electron microscope (SEM). Before image capturing, the sample powders were dispersed on a

conductive adhesive carbon tab placed on a SEM mount. All SEM images were obtained from secondary electrons with 5 kV of accelerating voltage. Elemental composition and distribution of a sample is determined using a NORAN System 7 X-ray microanalysis (EDS) system from Thermo Fisher Scientific.

The specific Brunauer-Emmett-Teller (BET) surface area and pore volume of selected materials were determined with N_2 adsorption/desorption isotherms obtained at approximately -196°C using ASAP 2460 (Micromeritics Instrument Corp) after out-gassing under vacuum for 6 h at 200°C.

X-ray diffraction (XRD) patterns were collected on a Philips PW 3040/60 powder diffractometer using Cu Kα radiation. The working voltage of the instrument was 40 kV and the current was 40 mA. The intensity data were collected at 25°C in a 2θ range from 20° to 90° with a scan rate of 0.1°/s.

The reduction properties of Ni/Cu composite materials were measured by means of temperature-programmed reduction (TPR) techniques. A 10-mg sample was placed in a quartz reactor which was connected to a conventional TPR apparatus, the reactor was heated from room temperature to 900°C at a heating rate of 10°C/min and the amount of H_2 uptake during the reduction was measured by a thermal conductivity detector (TCD).

X-ray photoelectron spectroscopy (XPS) experiments were conducted using a Thermo Escalab 250Xi spectrometer with monochromatized Al Kα 1486.6 eV. The pressure in the analysis chamber during experiments was kept at 1×10^{-10} mbar. A hemispherical electron-energy analyzer working at a pass energy of 20 eV was used to collect core-level spectra. Charge effects were corrected by using the C 1s peak at 284.8 eV. Peak positions were detected and corrected by the instrument.

3. Results and Discussion

3.1. Characterization of composites

Morphologies of fresh catalysts with different CuO content were imaged using SEM, as shown in

Figures 3(a-d). Larger grains are observed to form and grow on the rough surface of the catalyst with higher CuO content, and these grains gathered and became lumps, especially for the sample of Cu5Ni12. Figures 3(e-h) show the surface morphologies of catalysts calcined at various temperatures. When the preparation temperature is higher, more apparent sintering of grains is present on the surface, indicating a gradual aggregation of active components with a non-uniform distribution.

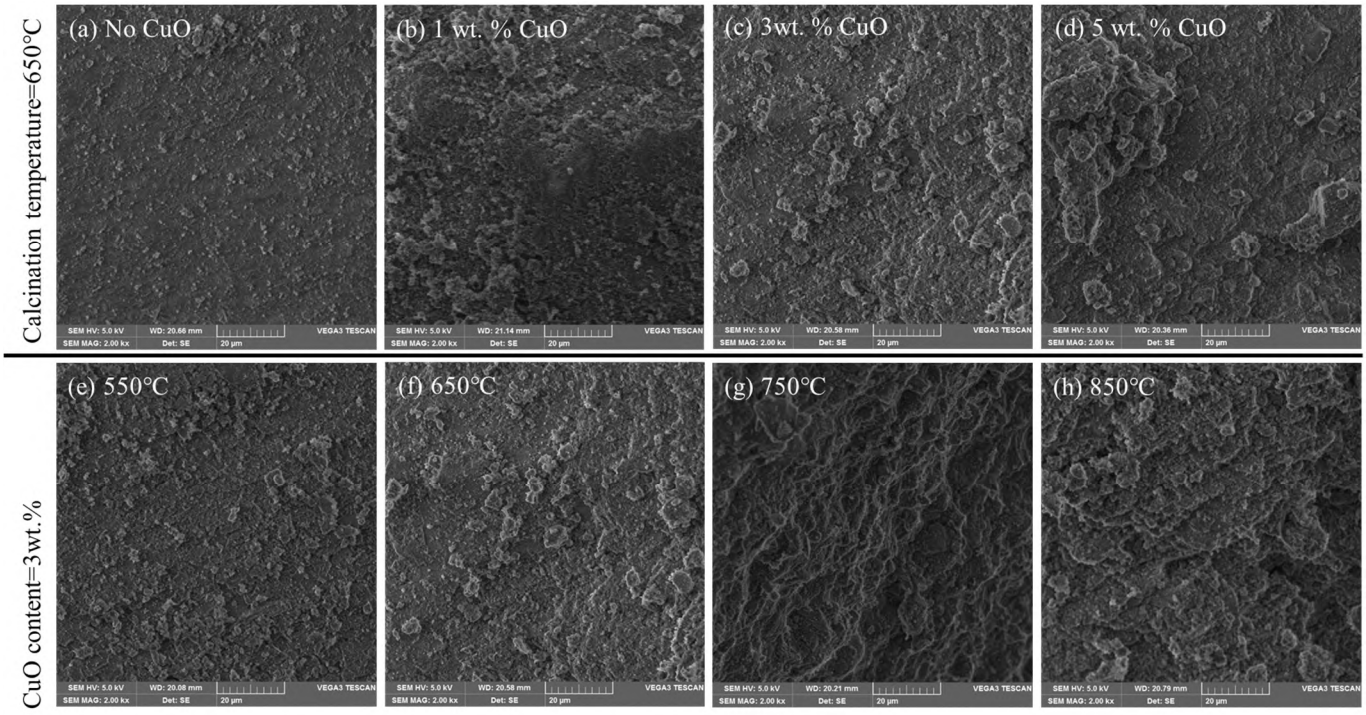

Figure 3. SEM images of fresh catalysts with different CuO contents: (a) Ni12, (b) Cu1Ni12, (c) Cu3Ni12, (d) Cu5Ni12, and Cu3Ni12 prepared at different calcination temperatures: (e) 550°C, (f) 650°C, (g) 750°C, (h) 850°C.

Typical samples were also tested by EDS technique and the content of Ni, Cu, Al and O on the random surface of the catalysts is shown in Table 1. It is seen that test contents of elements from EDS are almost the same to their theoretical values. More visualized results could also be seen from the element distribution images, as shown in Figure 4, which demonstrated that all the catalysts tested have a uniform distribution of Ni and Cu on the support.

Table 1. EDS semi-quantitative analysis data of surface element content (wt.%).

Element	Ni12	Cu1Ni12	Cu3Ni12	Cu5Ni12	Cu3Ni12 (550°C)	Cu3Ni12 (750°C)	Cu3Ni12 (850°C)
Cu		0.74	2.63	5.96	3.81	2.53	2.94
Ni	12.57	9.34	10.80	9.30	13.04	10.82	8.61
Al	41.20	44.55	43.69	42.33	42.29	43.09	41.61
O	46.23	45.37	42.88	42.42	40.87	43.56	46.84

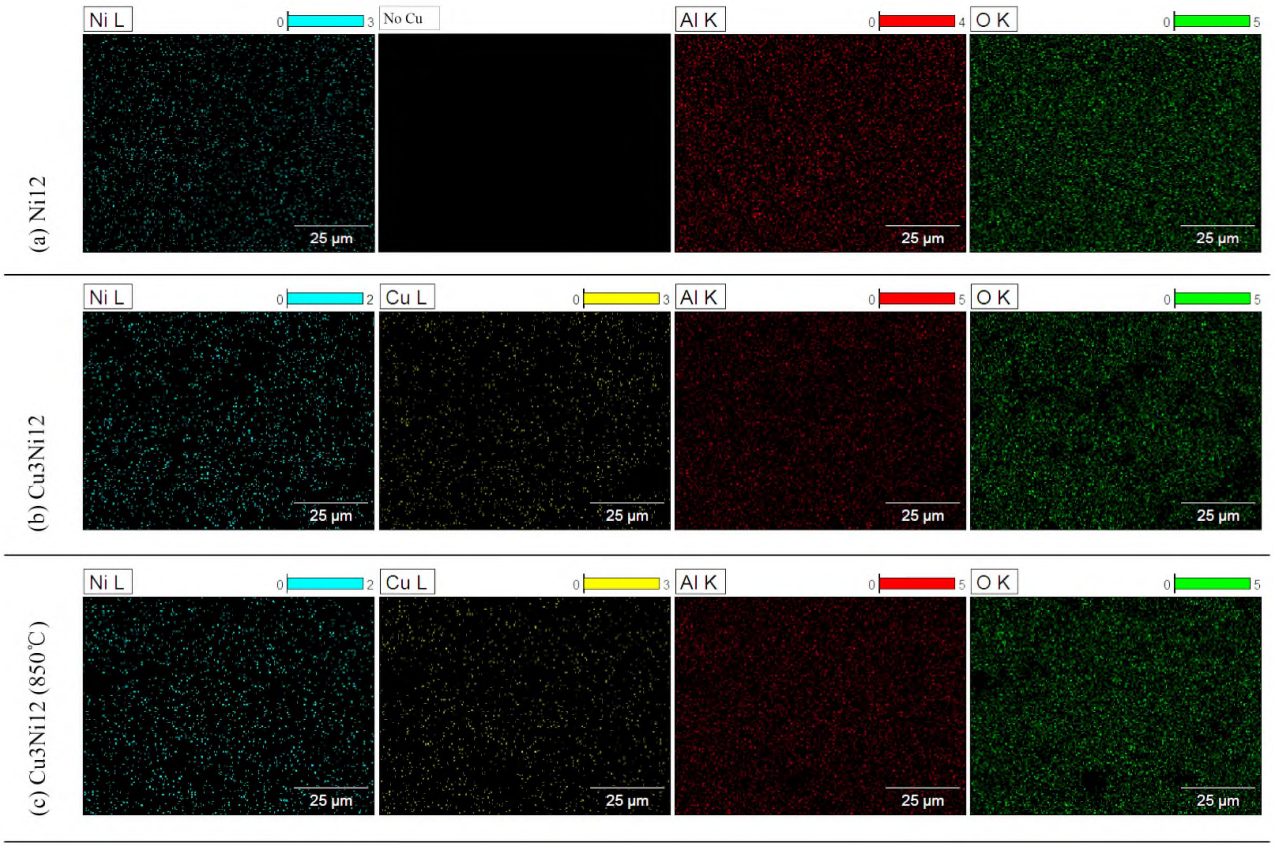

Figure 4. EDS element distribution images of (a) Ni12, (b) Cu3Ni12, and (c) Cu3Ni12 (850°C).

Microscopic pore structure of various samples was characterized and parametric data are summarized in Table 2. The pore size distribution curve is also presented, as shown in Figure 5. We can see that the pore size distribution peak of all catalysts with copper addition is slightly shifted toward smaller pores. However, with CuO content increasing from 0 to 5 wt.% and calcination

temperature varying from 500°C to 850°C, there is only a slight change in the specific surface area, average pore volume and pore size.

Table 2. Textural properties of fresh catalysts with different CuO contents and calcination temperatures**.**

Sample	BET surface area (m^2/g)	Average pore volume (g/cm^3)	Average pore size (nm)
Ni12	151.94	0.57	14.03
Cu3Ni12	153.01	0.53	11.59
Cu5Ni12	155.54	0.54	13.22
Cu3Ni12 (500°C)	160.63	0.51	10.75
Cu3Ni12 (750°C)	149.76	0.54	12.52
Cu3Ni12 (850°C)	152.11	0.52	13.02

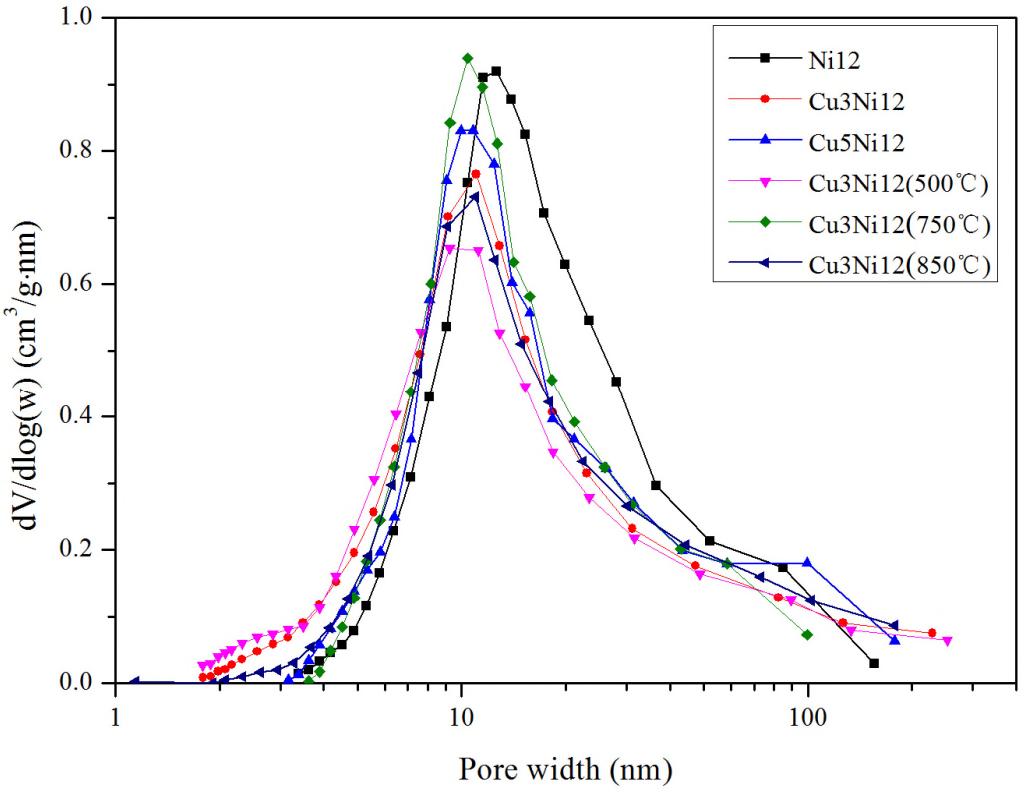

Figure 5. Pore size distribution of fresh catalysts with different CuO contents and calcination temperatures.

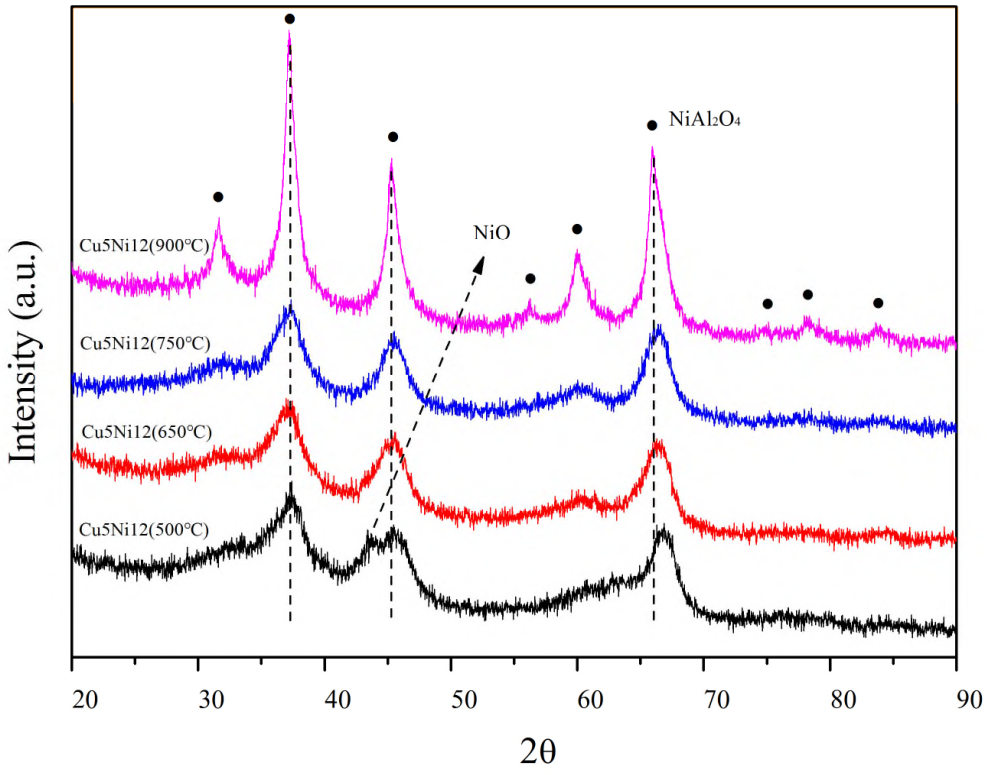

Figure 6. XRD patterns for the fresh catalysts prepared at different calcination temperatures.

Figure 6 shows XRD patterns of fresh catalysts (CuO content is fixed at 5 wt.%) prepared at calcination temperatures ranging from 500°C to 900°C. When the calcination temperature is lower than 500°C, the NiO phase can be found at 43.6°. However, with the rise of calcination temperature, only $NiAl_2O_4$ could be observed with its crystallinity gradually increased, especially for the sample of Cu5Ni12 (900°C). This suggests that the interaction between NiO and Al_2O_3 is enhanced at higher calcination temperatures.

3.2. Effect of CuO content on catalytic activity

Though Ni/Cu composites with a high CuO content (50 wt.%) were synthesized, no catalytic activity in the SMR process was observed in our fixed-bed reactor tests. Therefore, potential interaction between CuO and NiO components in Ca-Cu chemical looping was studied by varying CuO content within a low range of 0-5 wt.%. Figure 7(a) shows the gas product composition using Ni12 without addition of CuO. It can be seen that the concentrations of all gases hardly varied during the test. H_2,

CO and CO_2 concentrations were stabilized at about 72%, 20% and 4%, respectively, and the residual CH_4 concentration accounted for only 4% of the dry gas composition. For tests with various CuO contents, gas product compositions are shown in Figures 7(b), (c) and (d). It is seen that hydrogen concentration remained at 72% using Cu1Ni12, but decreased to 69% and 63% when CuO addition was raised to 3 wt.% and 5 wt.%, respectively. The CO concentration is about 14%, 10% and 11% respectively, which is lower than the corresponding value using only Ni12. And the CO_2 concentration is around 7%, 9% and 6%, respectively, which are higher than that for the Ni12 test. More significantly, concentrations of the residual CH_4 rose dramatically with the increase of CuO content from 0 wt.% to 1 wt.%, 3 wt.% and 5 wt.%, going up to 7%, 11% and 20%, respectively. This suggests that the extent of the SMR reaction was badly hindered as the content of CuO rose.

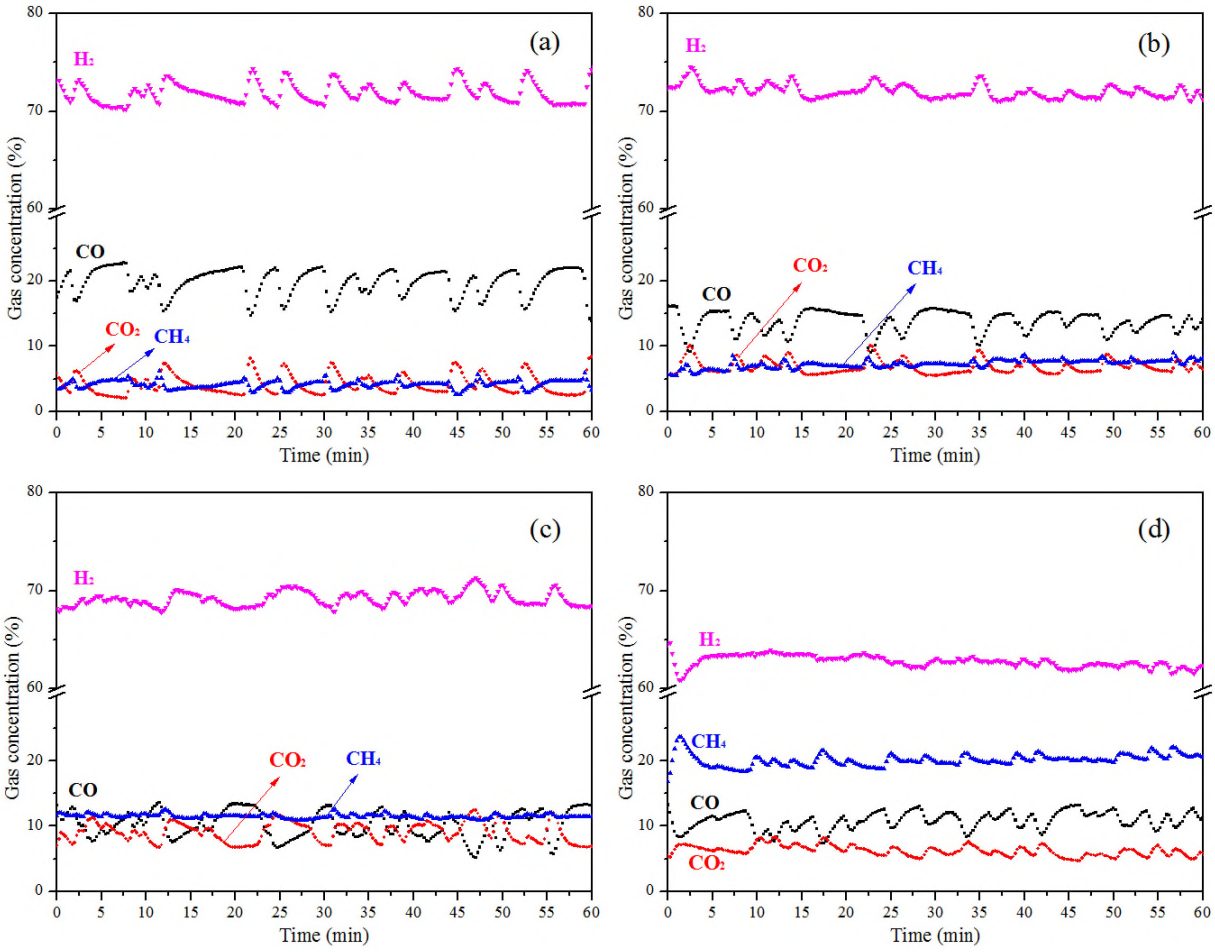

Figure 7. Product gas composition (dry basis) of SMR using (a) Ni12, (b) Cu1Ni12, (c) Cu3Ni12, and (d) Cu5Ni12. (Reaction conditions: 1atm, 650°C, molar ratio of $H_2O/CH_4 = 4$)

To show the impact of CuO on Ni-based catalysts more clearly, the conversion of CH_4, and selectivity of CO, CO_2 and H_2 are summarized in Figure 8. We can see that with the increase of CuO content from 0 to 1, 3 and finally 5 wt. %, the selectivity of H_2, which stands for the proportion of H_2 in the product gas (CO, CO_2 and H_2), was almost stabilized at the same value around 78%. However, CO selectivity decreased from 20.6% to 14.9%, 11.5% and 13.6%, respectively. By contrast, CO_2 selectivity increased from 4.3% to 7.4%, 10.2% and 7.8%, and the conversion of CH_4 decreased monotonically from 85.2% to 73.8%, 62.5% and 48.9%, respectively. Combined with the results demonstrated in Figures 7(a-d), it is very clear that the presence of CuO, even in small amounts, can greatly hinder the activity of Ni-based catalyst in the SMR reaction for converting CH_4 to produce H_2. And the greater addition of CuO results in a higher residual CH_4 concentration and a lower H_2 fraction.

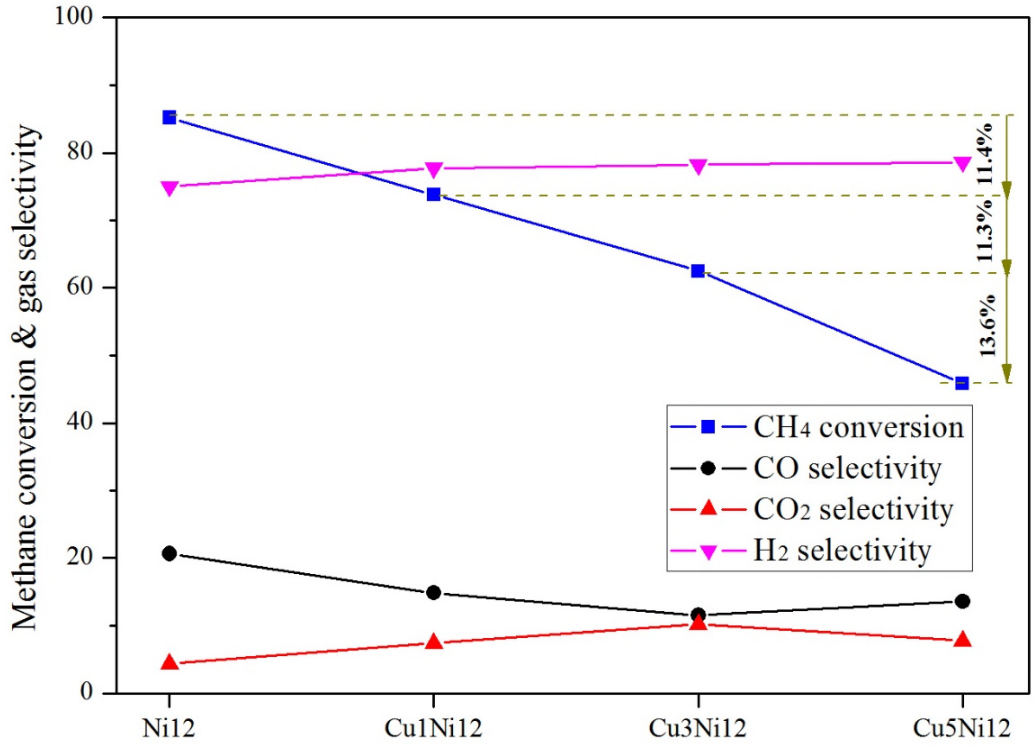

Figure 8. Methane conversion and gas selectivity in SMR with CuO content varying from 0 to 5 wt.%.

3.3. Effect of calcination temperature on catalytic activity

To further study the interaction between CuO and Ni-based catalysts, calcination temperature during

sample preparation was varied from 550°C to 850°C, and the product gas composition as a function of reaction time is depicted in Figures 9(a-c). When Cu3Ni12 was calcined at 550°C, it is seen that the real-time H_2, CO and CO_2 concentration were constant at around 70%, 15%, and 7%, respectively, and the concentration of CH_4 was about 8%. When calcination temperature was increased to 750°C and 850°C, as shown in Figures 9(b) and (c), the concentration of H_2 in the production gas declined to 59% and 57%, the mole fraction of CO decreased to 9% and 6%, and the concentration of CO_2 is 6% and 9%, respectively, while the molar fraction of unreacted CH_4 increased to 25% and 27%. The conversion of CH_4 and gas selectivity as a function of calcination temperature of Cu3Ni12 are demonstrated in Figure 9(d). This shows that the selectivity of H_2, CO and CO_2 were almost constant, but there was an apparent decline of CH_4 conversion from 70% at 550°C to 36% at 850°C. These results indicate that higher calcination temperature could largely deteriorate the activity of Ni/Cu catalyst in the SMR reaction for converting CH_4 to produce H_2.

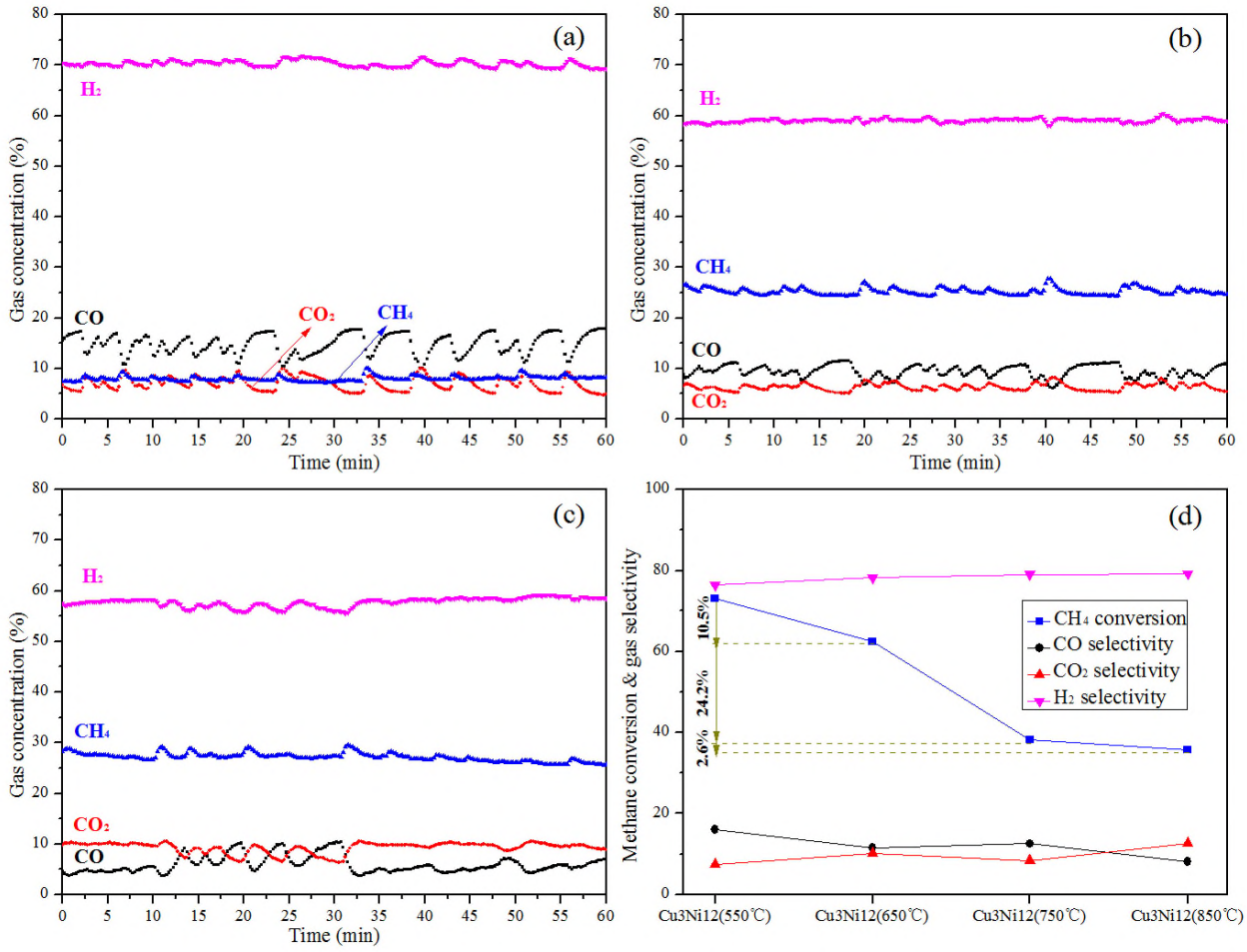

Figure 9. Product gas composition (dry basis) of SMR using Cu3Ni12 calcined at (a) 550°C, (b) 750°C, and (c) 850°C, and (d) methane conversion and gas selectivity. (Reaction conditions: 1 atm, 650°C, molar ratio of $H_2O/CH_4 = 4$).

3.4. Mechanism of the CuO/NiO interaction

To better understand the interaction between CuO and NiO, the shift of reduction temperature of catalysts was studied by the TPR method. Figure 10(a) shows the TPR spectra of fresh samples with different CuO content, while keeping the fraction of NiO at 12 wt.%. It can be seen that Ni12 has a single peak β_3 at around 760°C, which can be assigned to $NiAl_2O_4$.[26, 27] With the addition and content increase of CuO, the peak was kept but its position was observed to move slightly towards the low-temperature side. In other words, the existence of CuO could accelerate the reduction rate of $NiAl_2O_4$ to some extent,[28] and this effect is proportional to the contact area between NiO and CuO. At the same time, a new small peak β_2 appeared at 600°C in Cu3Ni12, which can be attributed to the reduction of NiO that has intimate contact with γ-Al_2O_3,[29] referred to as "intimate NiO". Most notably, there is a new peak β_1 at around 450°C appearing in Cu5Ni12, relating to the reduction of NiO at a free state that is referred to as "bulk NiO".[30, 31] On the other hand, with the CuO load increasing, the α peak of CuO shifts to a lower temperature.[32] In brief, The contact area between NiO and CuO is expanding with CuO content increasing from 0 to 5 wt.%.

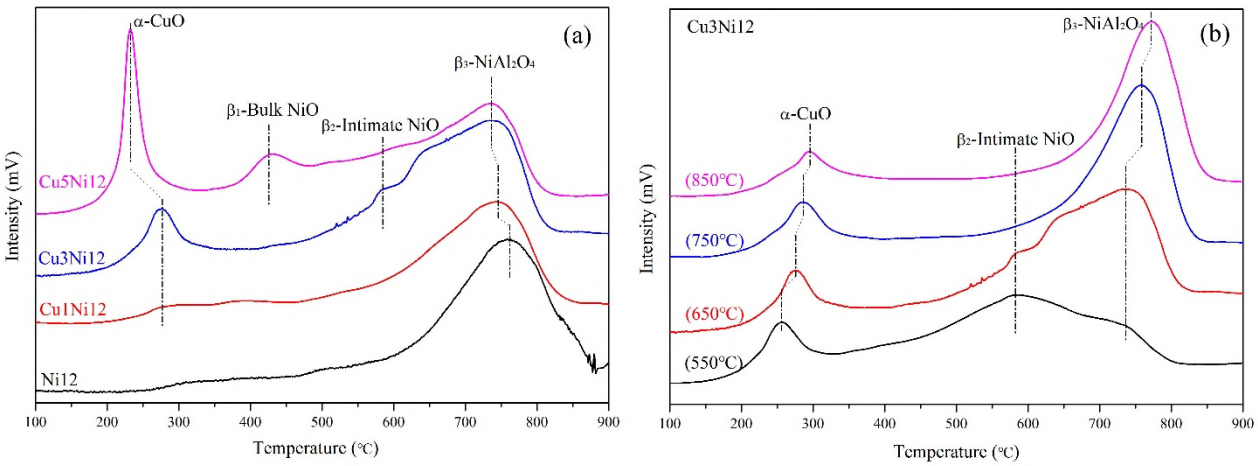

Figure 10. TPR of the (a) fresh catalysts prepared at 650°C with various CuO contents, and (b) fresh Cu3Ni12 prepared at different calcination temperatures.

Figure 10(b) shows the TPR of Cu3Ni12 prepared at different calcination temperatures. It can be seen that Cu3Ni12 calcined at 550°C has a very clear peak β_2 of 'intimate NiO', but the peak β_3 of $NiAl_2O_4$ is not so obvious. Increasing the calcination temperature caused peak β_3 of $NiAl_2O_4$ to move to the position with a higher reduction temperature. Meanwhile, the peak β_2 of 'intimate NiO' gradually disappeared and was replaced by $NiAl_2O_4$ when the temperature was higher than 750°C. The reason for this behaviour is that the higher calcination temperature improves the crystallinity of catalysts and strengthens the interaction between NiO and Al_2O_3, which can also be seen in XRD results, thus NiO becomes more difficult to be reduced. On the other hand, the peak of CuO was also shifted from 255°C to 295°C when increasing the calcination temperature. This suggests that the dispersion of CuO becomes worse due to the well-known easy-aggregation characteristic of CuO. Interestingly, though crystal $CuAl_2O_4$ was reported to form above 700°C,[32] the reduction peak of $CuAl_2O_4$ is not found in our TPR test even when the calcination temperature reached 850°C.

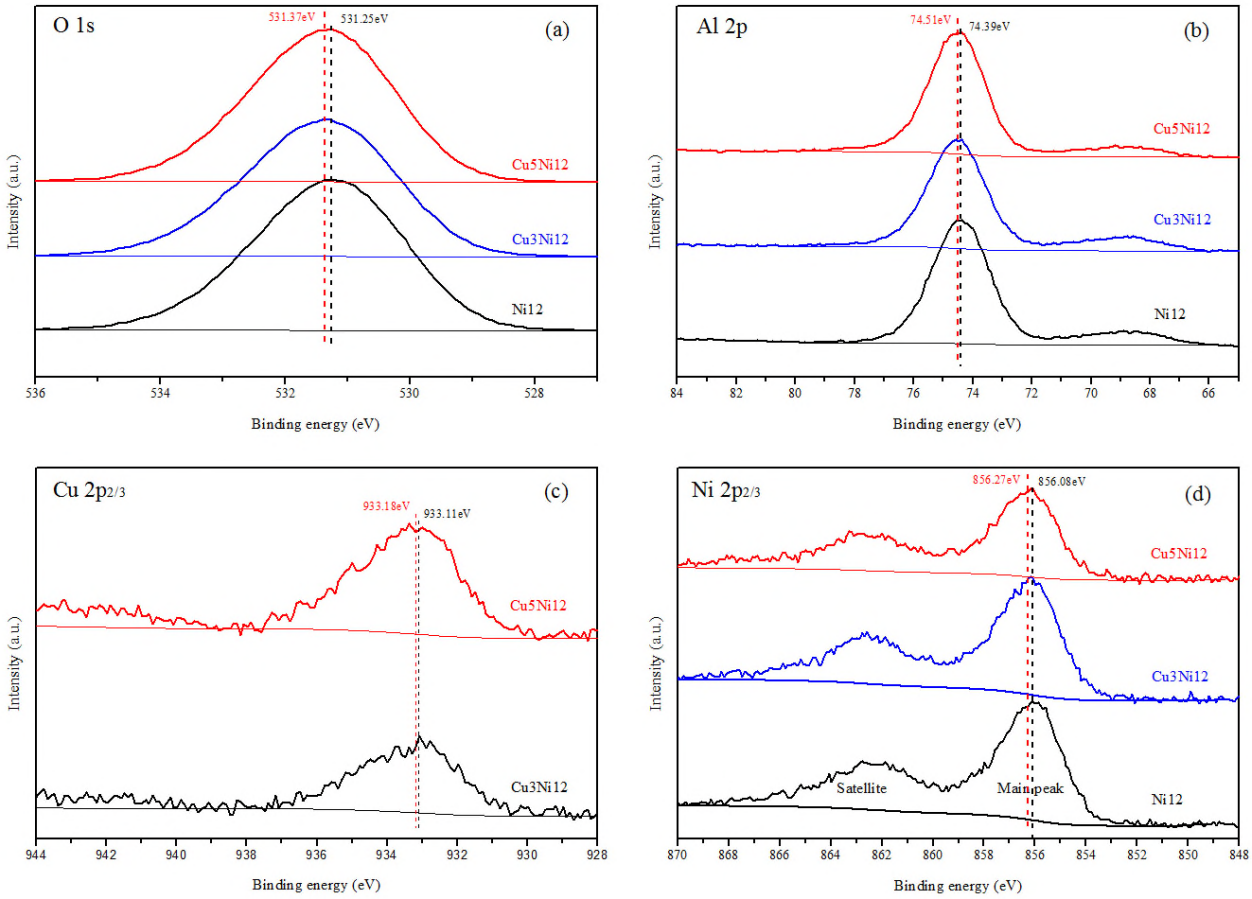

Figure 11. XPS spectra of fresh samples Ni12, Cu3Ni12 and Cu5Ni12. (a) O 1s, (b) Al 2p, (c) Cu $2p_{3/2}$ and (d) Ni $2p_{3/2}$.

In addition, the XPS technique is applied in the work to obtain the binding energy (BE) value of elements, in order to confirm the solid solution form and the interaction of CuO/NiO. Figures 11(a) and (b) show the O 1s and Al 2p core level spectra of catalysts with different additions of CuO. It should be noted that the γ-Al_2O_3 support accounts for 83 wt. %-88 wt. % of catalyst, thus the valence state of Al_2O_3 dominates the BE feature of O 1s and Al 2p. After the addition of CuO, the BE feature of both O1s and Al 2p increases marginally. As shown in Table 3, the BE values of O 1s and Al 2p increased from 531.25 eV and 74.39 eV to around 531.37 eV and 74.51 eV, respectively. Together with the results from the TPR test, it can be concluded that CuO addition resulted in some replacement of $NiAl_2O_4$ by separate NiO and Al_2O_3.

Table 3. XPS experimental BE values of samples with different contents of CuO and the reference Cu $2p_{3/2}$, Ni $2p_{3/2}$ (eV).

Sample	Ni $2p_{3/2}$	Cu $2p_{3/2}$	O 1s	Al 2p
Ni12	856.08		531.25	74.39
Cu3Ni12	856.18	933.11	531.38	74.53
Cu5Ni12	856.27	933.18	531.37	74.51
CuO		933.8[33]		
$CuAl_2O_4$		935.0[34]		
NiO	854.5[35]			
$NiAl_2O_4$	856[36]			

Cu $2p_{3/2}$ core level spectra of catalysts with different CuO contents are depicted in Figure 11(c), and Cu3Ni12 and Cu5Ni12 were shown to have the Cu $2p_{3/2}$ main peak at 933.11 eV and 933.18 eV, respectively. Compared with the standard BE value of $CuAl_2O_4$ in Table 3, it is confirmed that all CuO exists in the bulk form, and there is no intimate interaction between CuO and Al_2O_3. Figure 11(d) shows the Ni $2p_{3/2}$ XPS spectra of catalysts, and it can be seen that BE value of Ni $2p_{3/2}$ is around 856.18±0.1 eV, corresponding to the form $NiAl_2O_4$. Though fresh catalysts are all kept at 12 wt.% NiO content, BE peak of Ni $2p_{3/2}$ was seen to shift slightly higher upon the addition of more CuO. The net increase of BE is 0.19 eV from Ni12 to Cu5Ni12 with a 5 wt.% CuO increment, indicating that the electron density of Ni species is depleted with increasing CuO in the catalysts. It is probable that the Cu species formed some kind of chemical interaction with the Ni species, thus the shielding effect of the outer electrons is weakened.

On the basis of catalytic testing and materials characterization, the discussion is put forward for the mechanism of NiO/CuO interaction. Thus, a model was proposed to represent what the actual surface

of the alloy particles may look like with different CuO loadings, as shown in Figure 11. When there is no CuO, as shown in Figure 12(a), the most active component exists in the form of $NiAl_2O_4$ which is uniformly dispersed on the support surface. When 1 wt.% of CuO was added into the catalyst, it can be presumed by TPR and XPS that most Cu exists in the form of CuO crystal instead of $CuAl_2O_4$, as shown in Figure 12(b); CuO most likely formed on the surface of $NiAl_2O_4$ and probably has minimal contact with the surface of Al_2O_3. When CuO content was increased to 3 wt.%, the BE value of Ni $2p_{3/2}$ also rose, indicating that the amount of CuO on $NiAl_2O_4$ surface became much greater, as shown in Figure 12(c). The aggregation of CuO probably blocked the growth of $NiAl_2O_4$, and NiO has to grow on a new surface, which is supported by the "intimate NiO", as found in the TPR test. When the content of CuO further increased to 5 wt.%, the BE value of Ni $2p_{3/2}$ increased similarly. In other words, the formation of $NiAl_2O_4$ was further restricted, and bulk NiO was formed on the surface, as shown in Figure 12(d). In brief, with the increase of CuO, its aggregation on the active surface becomes more pronounced, which causes a decrease of the contact area available for Ni. What is worse, the blocking effect of CuO caused redistribution of the Ni component and the appearance of "intimate NiO" and "Bulk NiO" further damaged its catalytic activity in the SMR process.

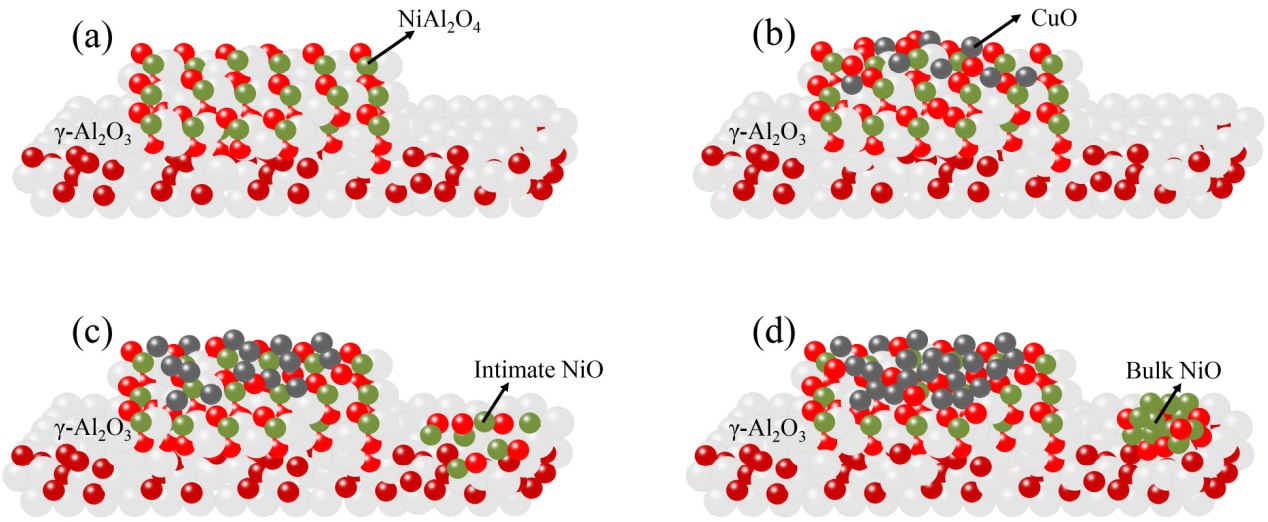

Figure 12. Proposed model for Ni-Al_2O_3 catalysts with CuO addition from 0 wt.% to 5 wt.%.

Though the interaction between NiO and Al_2O_3 is found to strengthen under a higher calcination temperature from the TPR results, it is not the main reason for the decline of catalyst activity. It is predicted that the poorer CuO dispersion and the decreasing contact area that available for Ni were the main contributors, which could be easily verified by the observed apparent shifting of α (CuO) and β_3 ($NiAl_2O_4$) reduction peaks towards higher temperature when catalysts were prepared under a higher temperature.

3.5. Arrangement of Cu-based oxygen carriers and Ni-based catalysts

To avoid the negative effect of CuO on SMR activity of Ni-based catalyst, an arrangement of particles containing Cu-based oxygen carriers and Ni-based catalysts separately rather than in intimate contact in one particle, was proposed and tested in this work. Both Cu-based material and Ca-Cu-based material were prepared by the co-precipitation method as typical materials in Ca-Cu looping. CuO/Al_2O_3 particles have a high CuO content of 75 wt.%, and Ca-Cu-based particles contains 63.76 wt.% CuO, 11.24 wt.% CaO and 25 wt.% Al_2O_3, which are identified as Cu75 and Cu64Ca, respectively. The proportion of Cu64Ca is determined based on the energies of reactions 3 and 5, assuming that energy can be balanced in the regenerator between the exothermic reduction of CuO with CH_4 and the endothermic calcination of $CaCO_3$.

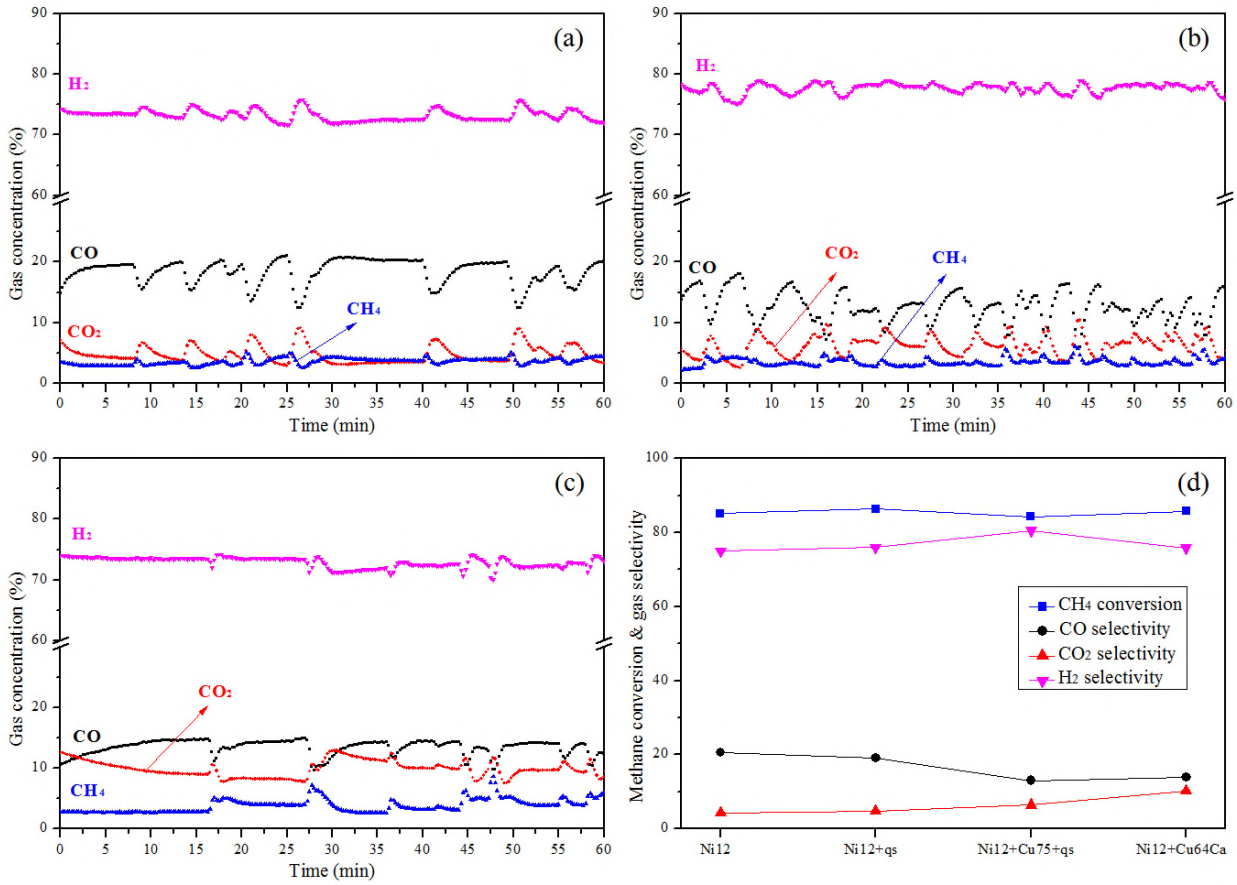

Figure 13. Product gas composition (dry basis) in SMR of (a) Ni12 + quartz sand, (b) Ni12 + Cu75 + quartz sand, and (c) Ni12 + Cu64Ca, and their (d) methane conversion and gas selectivity (Reaction conditions: 1 atm, 650°C, molar ratio of $H_2O/CH_4 = 4$).

The catalyst test is performed using the same conditions as in previous experiments. To minimize the potential gas diffusion effect in the reactor, quartz sand with the same size is introduced as an inert bed material. Three experiments were conducted: (1) 1 g Ni12 + 1 g quartz sand, (2) 1 g Ni12 + 0.85 g Cu75 + 0.15 g quartz sand, and (3) 1 g Ni12 + 1 g Cu64Ca, and the results are summarized in Figure 13. It can be seen that the H_2 concentration is above 72% and the residual CH_4 is kept at or below 5% in all 3 experimental tests, demonstrating good SMR catalytic performance with CH_4 conversion stabilized at around 85%. The results show that both Cu75 and Cu64Ca worked similarly to the catalyst without CuO. Therefore, the segregation of NiO from intimate contact with CuO can completely eliminate the mutual interaction and retain their individual functions in Ca-Cu chemical looping for

H_2 production.

4. Conclusions

This work focused on exploring the Ni/Cu multifunctional composite in the Ca-Cu chemical looping for hydrogen production process. It is reported for the first time, to our knowledge, that the Ni/Cu composite exhibits poor compatibility, and the activity of Ni/Cu catalyst sharply declines with increasing CuO content or calcination temperature. With the help of TPR and XPS testing, the metal phase of NiO and CuO was analyzed, and it was observed that part of NiO phase was transformed from $NiAl_2O_4$ into "intimate NiO" and finally "Bulk NiO" with increased CuO content. The BE value of Ni $2p_{3/2}$ rose by 0.19 eV from Ni12 to Cu5Ni12. It is suggested that when there is intimate contact between CuO/NiO, expanding aggregation of CuO on the active surface would occur with the increase of CuO content and result in a decrease of the available contact area for Ni. A higher calcination temperature during catalyst preparation could also exacerbate this problem. Eventually, an arrangement of mixed particles with individual components that could avoid the intimate contact of CuO/NiO was suggested and examined, and it demonstrated a good SMR catalytic performance with CH_4 conversion stabilized at around 85%.

Acknowledgements

The authors are grateful for the financial support from the National Natural Science Foundation of China (No. 51606018), Chongqing Basic Science and Advanced Technology Research Program (No. cstc2017jcyjAX0324) and Key Laboratory of Low-grade Energy Utilization Technologies and Systems of Ministry of Education (No. LLEUTS-2016004).

References

[1] Harrison DP. Sorption-Enhanced Hydrogen Production: A Review. Industrial & Engineering Chemistry Research. 2008;47:6486-501.

[2] Bhat SA, Sadhukhan J. Process intensification aspects for steam methane reforming: An overview. AIChE Journal. 2009;55:408-22.

[3] Abanades JC, Arias B, Lyngfelt A, Mattisson T, Wiley DE, Li H, et al. Emerging CO_2 capture systems. International Journal of Greenhouse Gas Control. 2015;40:126-66.

[4] Lyon RK. Method and apparatus for unmixed combustion as an alternative to fire. Google Patents; 1996.

[5] Abanades JC, Murillo R, Fernandez JR, Grasa G, Martínez I. New CO_2 Capture Process for Hydrogen Production Combining Ca and Cu Chemical Loops. Environmental Science & Technology. 2010;44:6901-4.

[6] Fernandez JR, Abanades JC, Grasa G. Modeling of sorption enhanced steam methane reforming—Part II: Simulation within a novel Ca/Cu chemical loop process for hydrogen production. Chemical Engineering Science. 2012;84:12-20.

[7] García-Lario AL, Martínez I, Murillo R, Grasa G, Fernández JR, Abanades JC. Reduction Kinetics of a High Load Cu-based Pellet Suitable for Ca/Cu Chemical Loops. Industrial & Engineering Chemistry Research. 2013;52:1481-90.

[8] Qin C, Feng B, Yin J, Ran J, Zhang L, Manovic V. Matching of kinetics of $CaCO_3$ decomposition and CuO reduction with CH_4 in Ca–Cu chemical looping. Chemical Engineering Journal. 2015;262:665-75.

[9] Qin C, Yin J, Feng B, Ran J, Zhang L, Manovic V. Modelling of the calcination behaviour of a uniformly-distributed $CuO/CaCO_3$ particle in Ca–Cu chemical looping. Applied Energy. 2016;164:400-10.

[10] Mattisson T. Materials for chemical-looping with oxygen uncoupling. ISRN Chemical Engineering. 2013;2013.

[11] Khzouz M, Wood J, Pollet B, Bujalski W. Characterization and activity test of commercial Ni/Al_2O_3, $Cu/ZnO/Al_2O_3$ and prepared $Ni–Cu/Al_2O_3$ catalysts for hydrogen production from methane and methanol fuels. International Journal of Hydrogen Energy. 2013;38:1664-75.

[12] Zhao M, Shi J, Zhong X, Tian S, Blamey J, Jiang J, et al. A novel calcium looping absorbent incorporated with polymorphic spacers for hydrogen production and CO_2 capture. Energy & Environmental Science. 2014;7:3291-5.

[13] He D, Qin C, Manovic V, Ran J, Feng B. Study on the interaction between CaO-based sorbents and coal ash in calcium looping process. Fuel Processing Technology. 2017;156:339-47.

[14] Broda M, Kierzkowska AM, Müller CR. Application of the Sol–Gel Technique to Develop Synthetic Calcium-Based Sorbents with Excellent Carbon Dioxide Capture Characteristics. ChemSusChem. 2012;5:411-8.

[15] Kierzkowska AM, Pacciani R, Müller CR. CaO-Based CO_2 Sorbents: From Fundamentals to the Development of New, Highly Effective Materials. ChemSusChem. 2013;6:1130-48.

[16] Phromprasit J, Powell J, Assabumrungrat S. Metals (Mg, Sr and Al) modified CaO based sorbent for CO_2 sorption/desorption stability in fixed bed reactor for high temperature application. Chemical Engineering Journal. 2016;284:1212-23.

[17] Duan L, Su C, Erans M, Li Y, Anthony EJ, Chen H. CO_2 Capture Performance Using Biomass-Templated Cement-Supported Limestone Pellets. Industrial & Engineering Chemistry Research. 2016;55:10294-300.

[18] Adánez J, Gayán P, Celaya J, de Diego LF, García-Labiano F, Abad A. Chemical Looping Combustion in a 10 kW_{th} Prototype Using a CuO/Al_2O_3 Oxygen Carrier: Effect of Operating Conditions on Methane Combustion. Industrial & Engineering Chemistry Research. 2006;45:6075-80.

[19] Cho P, Mattisson T, Lyngfelt A. Comparison of iron-, nickel-, copper- and manganese-based oxygen carriers for chemical-looping combustion. Fuel. 2004;83:1215-25.

[20] Chanburanasiri N, Ribeiro AM, Rodrigues AE, Arpornwichanop A, Laosiripojana N, Praserthdam P, et al. Hydrogen Production via Sorption Enhanced Steam Methane Reforming Process Using Ni/CaO Multifunctional Catalyst. Industrial & Engineering Chemistry Research. 2011;50:13662-71.

[21] Broda M, Kierzkowska AM, Baudouin D, Imtiaz Q, Copéret C, Müller CR. Sorbent-Enhanced Methane Reforming over a Ni–Ca-Based, Bifunctional Catalyst Sorbent. ACS Catalysis. 2012;2:1635-46.

[22] Xu P, Zhou Z, Zhao C, Cheng Z. Catalytic performance of Ni/CaO-$Ca_5Al_6O_{14}$ bifunctional catalyst extrudate in sorption-enhanced steam methane reforming. Catalysis Today. 2016;259, Part 2:347-53.

[23] Manovic V, Wu Y, He I, Anthony EJ. Core-in-Shell CaO/CuO-Based Composite for CO_2 Capture. Industrial & Engineering Chemistry Research. 2011;50:12384-91.

[24] Qin C, Yin J, Liu W, An H, Feng B. Behavior of CaO/CuO Based Composite in a Combined Calcium and Copper Chemical Looping Process. Industrial & Engineering Chemistry Research. 2012;51:12274-81.

[25] Qin C, Yin J, Luo C, An H, Liu W, Feng B. Enhancing the performance of CaO/CuO based composite for CO_2 capture in a combined Ca–Cu chemical looping process. Chemical Engineering Journal. 2013;228:75-86.

[26] Molina R, Poncelet G. α-Alumina-Supported Nickel Catalysts Prepared from Nickel Acetylacetonate: A TPR Study. Journal of Catalysis. 1998;173:257-67.

[27] Lemonidou AA, Vasalos IA. Carbon dioxide reforming of methane over 5 wt.% Ni/CaO-Al_2O_3 catalyst. Applied Catalysis A: General. 2002;228:227-35.

[28] Roman A, Delmon B. Promoter and carrier effects in the reduction of NiOSiO_2. Journal of Catalysis. 1973;30:333-42.

[29] Hou Z, Yokota O, Tanaka T, Yashima T. Characterization of Ca-promoted Ni/α-Al_2O_3 catalyst for CH_4 reforming with CO_2. Applied Catalysis A: General. 2003;253:381-7.

[30] Hu C-W, Yao J, Yang H-Q, Chen Y, Tian A-M. On the Inhomogeneity of Low Nickel Loading Methanation Catalyst. Journal of Catalysis. 1997;166:1-7.

[31] Lee J-H, Lee E-G, Joo O-S, Jung K-D. Stabilization of Ni/Al_2O_3 catalyst by Cu addition for CO_2 reforming of methane. Applied Catalysis A: General. 2004;269:1-6.

[32] Luo M-F, Fang P, He M, Xie Y-L. In situ XRD, Raman, and TPR studies of CuO/Al_2O_3 catalysts for CO oxidation. Journal of Molecular Catalysis A: Chemical. 2005;239:243-8.

[33] Moretti G, Fierro G, Lo Jacono M, Porta P. Characterization of CuO–ZnO catalysts by X-ray photoelectron spectroscopy: Precursors, calcined and reduced samples. Surface and Interface Analysis. 1989;14:325-36.

[34] Strohmeier BR, Levden DE, Field RS, Hercules DM. Surface spectroscopic characterization of $CuAl_2O_3$ catalysts. Journal of Catalysis. 1985;94:514-30.

[35] Wagner CD. Handbook of x-ray photoelectron spectroscopy: a reference book of standard data for use in x-ray photoelectron spectroscopy: Physical Electronics Division, Perkin-Elmer Corp.; 1979.

[36] Lenglet M, Hochu F, Dürr J, Tuilier MH. Investigation of the chemical bonding in 3d8 nickel(II) charge transfer insulators (NiO, oxidic spinels) from ligand-field spectroscopy, Ni 2p XPS and X-ray absorption spectroscopy. Solid State Communications. 1997;104:793-8.